Digital Object Identifier (DOI): 10.1109/TIE.2017.2777419

IEEE Transactions on Industrial Electronics (Volume: 65, Issue: 7, July 2018)

Performance comparison of variable-angle phase-shifting carrier PWM techniques

Vito Giuseppe Monopoli
Youngjong Ko
Giampaolo Buticchi
Marco Liserre

Suggested Citation

V. G. Monopoli, Y. Ko, G. Buticchi and M. Liserre, "Performance Comparison of Variable-Angle Phase-Shifting Carrier PWM Techniques," in *IEEE Transactions on Industrial Electronics*, vol. 65, no. 7, pp. 5272-5281, July 2018.

Performance Comparison of Variable-Angle Phase-Shifting Carrier PWM Techniques

Vito Giuseppe Monopoli, *Member, IEEE*, Youngjong Ko, *Student Member, IEEE*, Giampaolo Buticchi, *Senior Member, IEEE*, and Marco Liserre, *Fellow, IEEE*

***Abstract*—This paper analyzes the performances of different carrier phase-shifting pulse width modulation (PWM) techniques to be used with a multilevel cascaded H-bridge converter in case of unbalanced operational conditions. In fact, in many practical applications, the ideal condition of equal dc voltages and equal reference signals for each H-bridge cannot be achieved. In such conditions, the conventional carrier phase-shifting PWM technique loses its harmonic canceling capabilities and then the multilevel ac voltage harmonic quality is deeply affected. To overcome this limit of the original technique, different variations have been proposed. All of them still rely on the carrier phase-shifting concept and propose to use a different value of the shifting angle for each carrier (unlike the original technique) whenever unbalanced operational conditions occur. In this paper, the three main solutions proposed over the last years to extend the capabilities of the carrier phase-shifting PWM technique are compared. The analysis is focused on a three-cell cascaded H-bridge converter. Simulation and experimental results are presented.**

***Index Terms*—Harmonic analysis, multilevel converters, pulse width modulation (PWM).**

I. Introduction

CASCADED multilevel converters have been considered over the last decade a consolidated solution for medium voltage drives and for a profitable interfacing of medium/high power loads and distributed generation sources to the electrical grid by means of a series of single-phase full-bridge power converters. Fig. 1 shows the general schematic of a cascaded multilevel converter. There are some applications of the cascaded H-bridge converter (CHB) where limited variations of both the amplitude and the frequency of the output voltage occur. In such cases, pulse width modulation (PWM) can be avoided and equivalent harmonic performance can be achieved through fundamental frequency selective harmonic elimination techniques also in presence of unbalanced dc voltages [1], [2]. Nevertheless, these techniques represent a practical approach only in case of limited output voltage regulation. In fact, whenever the range of variation of the output voltage is wide and rapid changes are required (e.g., motor drives), the PWM of the CHB becomes again a more viable solution [3]. One of the most used modulation techniques related to such a conversion topology is referred to as phase-shifting carrier PWM (PSC-PWM).

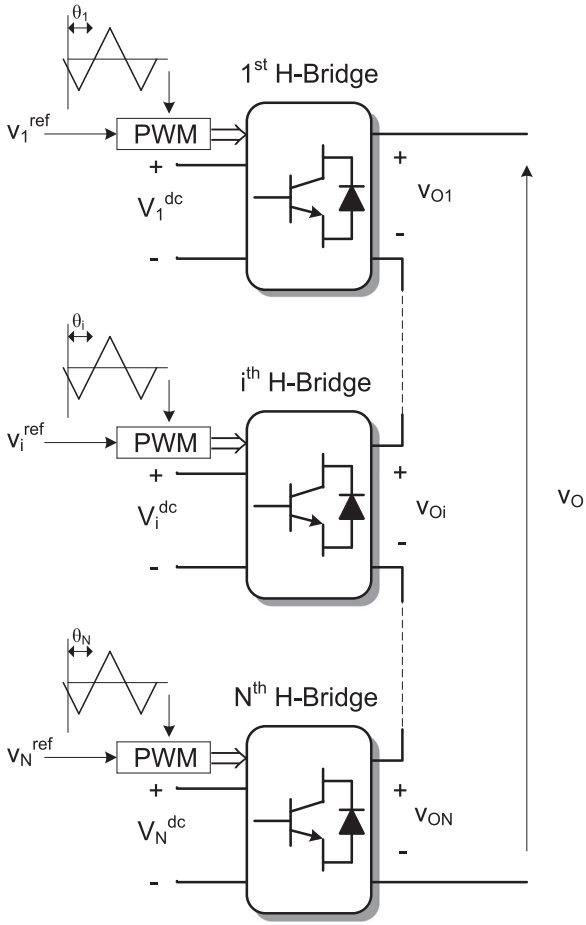

Fig. 1. Cascaded multilevel converter topology.

It allows us to reduce the weighted total harmonic distortion (WTHD) of the overall output voltage waveform by equally shifting the relative phase of the triangular carrier employed in each H-bridge. In fact, in case of N cascaded bridges, when car-

Manuscript received March 24, 2017; revised July 19, 2017; accepted November 5, 2017. Date of publication November 24, 2017; date of current version March 6, 2018. *(Corresponding author: Vito Giuseppe Monopoli.)*

V. G. Monopoli is with the Department of Electrical and Information Engineering, Politecnico di Bari, Bari 70126, Italy (e-mail: vitogiuseppe.monopoli@poliba.it).

Y. Ko and M. Liserre are with the Chair of Power Electronics, Christian-Albrechts Universität zu Kiel, Kiel 24143, Germany (e-mail: yoko@tf.uni-kiel.de; ml@tf.uni-kiel.de).

G. Buticchi is with the University of Nottingham Ningbo, Ningbo 315100, China (e-mail: giampaolo.buticchi@nottingham.edu.cn).

Color versions of one or more of the figures in this paper are available online at http://ieeexplore.ieee.org.

Digital Object Identifier 10.1109/TIE.2017.2777419

rier phase shifts of $(i-1)\pi/N$ are considered, optimal harmonic components cancellation up to the $2N$th carrier multiple occurs [3]. Nevertheless, the main limit with the PSC-PWM is that a perfectly balanced operation is required that means equal dc voltages and equal modulation indexes for all the cascaded bridges. This aspect deeply limits the cases where this technique can provide all its potentiality.

In fact, there are applications where the dc voltage levels are meant to be equal but voltage unbalancing occurs because of unequal power loading [4] or unequal losses among the cascaded bridges [5]. To face such issues some balancing control methods have been proposed in the literature. In particular, Dell'Aquila *et al.* [4] and Barrena *et al.* [6] propose to adjust the modulating signal, whereas Soto *et al.* [7] investigates the injection of voltage/current components. Moreover, PSC-PWM itself is inherently unbalancing and for this reason a pulse rotation technique must normally be applied.

In addition to the aforementioned cases, there are some applications that can be considered intentionally unbalanced [8] (asymmetric cascaded H-bridges), such as the CHB motor drive capable of regenerating with part of cells [9] and the grid connected multilevel converters that can integrate several kind of dc sources (photovoltaic, batteries, supercapacitors, etc.) and can manage different voltage levels [10]–[12]. In all these cases, the conventional PSC-PWM fails since the calculated phase-shifting angles do not allow the cancellation of harmonics up to the $2N$th carrier multiple anymore. To deal with these operational conditions an extension of PSC-PWM was proposed in [13]. It achieves the harmonic cancellation once again, and hence, the minimization of the overall output voltage WTHD, through an unequal and dynamically calculated carrier phase shifting that makes null the sum of particular harmonics produced by each bridge. This technique, formerly proposed in [13], has been reconsidered and extended in successive works. In fact, a more comprehensive analysis of the technique proposed in [13] is presented in [14]. It is still focused on the case with unbalanced dc voltages and equal modulating signals for all the H-bridges. In particular, details are provided about the harmonic cancellation capability and an upper limit for the equivalent switching frequency with asymmetrical carrier phase-shifting PWM is defined. Additionally, a technique that is still a modification of the conventional CPS-PWM is presented in [15] and it is meant for a cascaded H-bridges STATCOM. This solution is profitably applied in the case of equal dc voltages, which tend to become unbalanced because of different power levels managed by the H-bridges or different power losses. In this case, different modulating signals have to be used to implement the dc -link voltage balance control method and the conventional CPS-PWM as well as the technique proposed in [13] cannot be applied since a unique modulating signal has to be used for all the H-bridges. Finally, in [16], a method is presented, which uses the Fourier series of the pulses, produced in each PWM period by the H-bridges, to calculate the carrier phase-shifting angles. This technique allows the cancellation of the fundamental harmonics ($2f_{\mathrm{PWM}}$) related to the pulses of each H-bridge and, in this case, unequal modulating signals and unequal dc voltages can be managed.

In this scenario, this paper aims at comparing the performances of these three main variations of the CPS-PWM in order to assess, which is the one that fits better to the different kind of unbalanced conditions and to provide a means to make a suitable selection among them. To this purpose, advantages and drawbacks as well as harmonic cancellation capability and validity limits of each technique are presented in Section II. In Section III, the WTHD's performed by each technique under different unbalanced conditions and the relevant theoretical harmonic spectra are shown. The analysis is focused on a three-cell CHB converter. The results of experimental tests are presented in Section IV. Finally, conclusions are drawn in Section V.

II. PSC PWM Techniques Under Unbalanced Conditions

A. PSC PWM Technique A [13]

This variation to the original CPS-PWM is suitable mainly for unequal dc voltages and equal modulating signals for each bridge. This technique achieves a WTHD improvement through an unequal carrier phase shifting that allows a cancellation of the carrier harmonics and the sideband harmonics produced by each bridge and belonging to the same harmonic group around multiples of the carrier fundamental.

Under these conditions, a double Fourier integral analysis leads to the following expression for the output ac voltage of the CHB converter:

$$\begin{aligned} v_0(t) &= M\sum_{i=1}^{N} V_i^{\mathrm{dc}}\cos(\omega_o t) \qquad \text{Fundamental} \\ &+\tfrac{4}{\pi}\sum_{m=1}^{\infty}\sum_{n=-\infty}^{\infty}\tfrac{1}{2m}J_{2n-1}(m\pi M)\cos([m+n-1]\pi) \\ &\cdot\sum_{i=1}^{N} V_i^{\mathrm{dc}}\cos(2m\omega_c t+[2n-1]\omega_o t+2m\theta_i) \quad \text{Carriers} \\ &\qquad\qquad + \text{Sidebands} \end{aligned} \tag{1}$$

where M is the modulation index, N is the number of cascaded bridges, V_i^{dc} is the dc voltage of the ith converter, ω_0 is the pulsation of the modulating signal, m and n are indexes to account for baseband, carrier, and sideband harmonics, J_{2n-1} is the Bessel function of order $2n-1$, ω_c is the pulsation of the carrier signal, and θ_i is the carrier phase of the ith converter.

In order to make null, the sum of the harmonics with the same harmonic order produced by each bridge, the following condition must be met:

$$\sum_{i=1}^{N} V_i^{\mathrm{dc}}\cos(2m\omega_c t+[2n-1]\omega_o t+2m\theta_i)=0 \tag{2}$$

which can be re-written as

$$\begin{cases} \sum_{i=1}^{N} V_i^{\mathrm{dc}}\cos(2m\theta_i)=0 \\ \sum_{i=1}^{N} V_i^{\mathrm{dc}}\sin(2m\theta_i)=0 \end{cases} \tag{3}$$

where $2m\theta_i$ represents the phase of all the harmonics (i.e., carriers + sidebands) belonging to the mth carrier group produced by the ith converter. As the index n varies, from (1) is evident that the harmonics with the same harmonic order, produced by each bridge, vary their amplitude of the same quantity since the

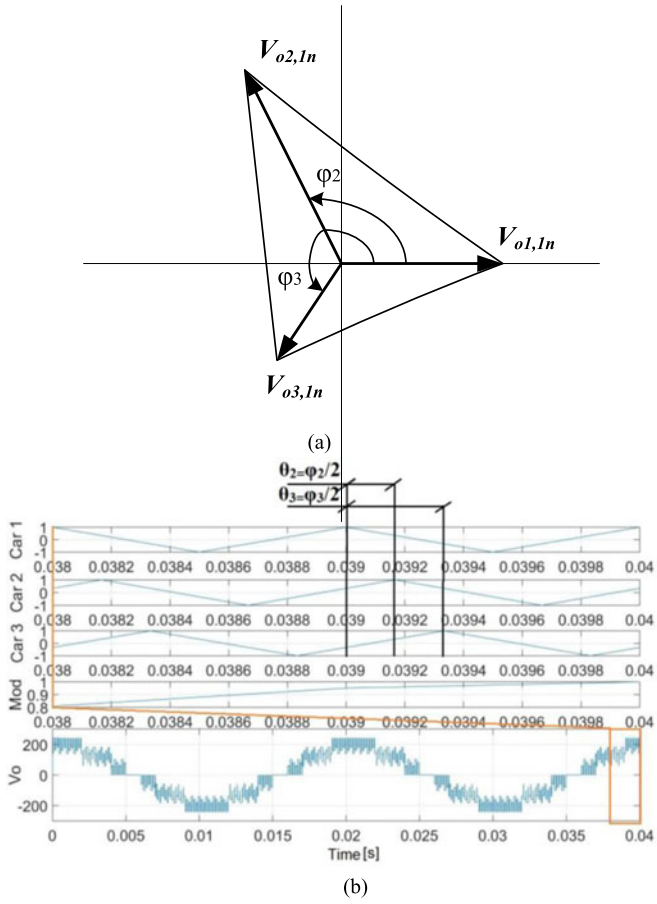

Fig. 2. (a) Harmonics belonging to the first carrier group produced by each bridge. (b) Multilevel output voltage, the three-phase-shifted carrier signals, and the modulating signal.

modulation index is equal. For this reason, the condition (3) is valid for all the harmonics belonging to the same carrier group. Therefore, the main advantage of this technique is that it is possible to cancel out all the harmonics of the same carrier group by fulfilling (3). Nevertheless, to set the problem in a closed form, assuming $\theta_1 = 0, N-1$ degrees of freedom (i.e., θ_i) can only satisfy $N-1$ equations in (3) [12]. Consequently, there is a relationship between the number of bridges N and the number of harmonic carrier groups m that are cancelled out in the converter output voltage. If N is odd, (3) is determined and $m_{\max} = (N-1)/2$. While, if N is even, (3) is undetermined and $m_{\max} = (N-2)/2$.

Considering the case $N = 3$, only the harmonics belonging to the first carrier group produced by the three bridges (i.e., $V_{oi,1n}$) can sum up to zero if proper phase shift angles are applied as shown in Fig. 2(a). The multilevel output voltage, the three phase-shifted carrier signals and the modulating signal are shown in Fig. 2(b).

In this case, (3) can be written as

$$\begin{cases} V_1^{\mathrm{dc}} + V_2^{\mathrm{dc}} \cos(\varphi_2) + V_3^{\mathrm{dc}} \cos(\varphi_3) = 0 \\ V_2^{\mathrm{dc}} \sin(\varphi_2) + V_3^{\mathrm{dc}} \sin(\varphi_3) = 0 \end{cases} \tag{4}$$

where $\varphi_2 = 2\theta_2$ and $\varphi_3 = 2\theta_3$ are, respectively, the displacement angles between of the harmonics of the second/third bridge and the harmonics of the first bridge belonging to the first carrier group (i.e., $m = 1$).

The solution to the equations in (4) is

$$\cos(\varphi_2) = \frac{1}{2}\left(\frac{-V_1^{\mathrm{dc}\,2} - V_2^{\mathrm{dc}\,2} + V_3^{\mathrm{dc}\,2}}{V_1^{\mathrm{dc}} V_2^{\mathrm{dc}}}\right)$$
$$\cos(\varphi_3) = \frac{1}{2}\left(\frac{-V_1^{\mathrm{dc}\,2} + V_2^{\mathrm{dc}\,2} - V_3^{\mathrm{dc}\,2}}{V_1^{\mathrm{dc}} V_3^{\mathrm{dc}}}\right). \tag{5}$$

Valid solutions for the displacement angles φ_2 and φ_3 are obtained only if the following conditions are met:

$$\left|V_1^{\mathrm{dc}} - V_2^{\mathrm{dc}}\right| \le V_3^{\mathrm{dc}} \le \left(V_1^{\mathrm{dc}} + V_2^{\mathrm{dc}}\right)$$
$$\left|V_1^{\mathrm{dc}} - V_3^{\mathrm{dc}}\right| \le V_2^{\mathrm{dc}} \le \left(V_1^{\mathrm{dc}} + V_3^{\mathrm{dc}}\right). \tag{6}$$

From (6) is evident that the validity region of this technique is influenced just by the dc voltage values of each bridge.

B. PSC PWM Technique B [15]

This variation to the original CPS-PWM is suitable for unequal dc voltages and unequal modulating signals for each bridge. This technique achieves a WTHD improvement through an unequal carrier phase shifting that allows a cancellation of selected sideband harmonics produced by each bridge and belonging to the same harmonic group around multiples of the carrier fundamental. Such harmonics are the ones that mostly influence the overall WTHD and are referred to as "main harmonics."

Under these conditions, a double Fourier integral analysis leads to the following expression for the output ac voltage of the CHB converter:

$$\begin{aligned} v_0(t) &= \sum_{i=1}^{N} M_i V_i^{\mathrm{dc}} \cos(\omega_o t) \qquad \text{Fundamental} \\ &+ \frac{4}{\pi} \sum_{m=1}^{\infty} \sum_{n=-\infty}^{\infty} \frac{1}{2m} \cos([m+n-1]\pi) \qquad \text{Carriers} \\ &\qquad + \text{Sidebands} \\ &\cdot \sum_{i=1}^{N} J_{2n-1}(m\pi M_i) V_i^{\mathrm{dc}} \cos(2m\omega_c t + [2n-1]\omega_o t + 2m\theta_i). \end{aligned} \tag{7}$$

In this case, the cancellation condition is not the same for all the harmonics belonging to the same carrier group and hence a cancellation of the harmonics of a whole group at the same time cannot be achieved anymore as it was in [13]. In fact, as the index n varies, from (7) is evident that the harmonics with the same harmonic order, produced by each bridge, do not vary their amplitude of the same quantity since the modulation indexes are unequal. Therefore, this technique makes null just the sum of the "main harmonics" that have $2f_c/f_o \pm 1$ harmonic order (i.e., $m = 1$ and $n = [0; 1]$). The amplitude of these main harmonics depends both on the dc voltage and on the modulation

index of each bridge as shown by the following expression:

$$V_i = \frac{2}{\pi} V_i^{\mathrm{dc}} J_{2n-1}(\pi M_i), \quad \text{for } i = 1, \ldots, N. \tag{8}$$

Considering the case $N = 3$, the sum of the main harmonics produced by each bridge is null if the following condition is met:

$$\begin{cases} V_1 + V_2 \cos(\varphi_2) + V_3 \cos(\varphi_3) = 0 \\ V_2 \sin(\varphi_2) + V_3 \sin(\varphi_3) = 0 \end{cases} \tag{9}$$

where $\varphi_2 = 2\theta_2$ and $\varphi_3 = 2\theta_3$ are, respectively, the displacement angles between the main harmonics of the second/third bridge and the main harmonic of the first bridge.

The solution to the equations in (8) is

$$\begin{aligned} \cos(\varphi_2) &= \frac{1}{2}\left(\frac{-V_1^2 - V_2^2 + V_3^2}{V_1 V_2}\right) \\ \cos(\varphi_3) &= \frac{1}{2}\left(\frac{-V_1^2 + V_2^2 - V_3^2}{V_1 V_3}\right). \end{aligned} \tag{10}$$

Valid solutions for the displacement angles φ_2 and φ_3 are obtained only if the following conditions are met:

$$\begin{aligned} |V_1 - V_2| &\le V_3 \le (V_1 + V_2) \\ |V_1 - V_3| &\le V_2 \le (V_1 + V_3). \end{aligned} \tag{11}$$

From (8) and (11) is evident that both the dc voltage values and the modulation index values of each bridge deeply influence the validity region of this technique.

C. PSC PWM Technique C [16]

This variation to the original CPS-PWM is suitable for unequal dc voltages and unequal modulating signals for each bridge. This technique achieves a WTHD improvement through an unequal carrier phase shifting that allows a cancellation of the harmonics produced by each bridge in case of unipolar modulation and placed at twice the carrier frequency. Unlike [13] and [15], this technique is not based on the double Fourier integral analysis. In this case, an analysis based on the Fourier series of the pulses produced by each bridge (with unipolar PWM) every T_{PWM} is carried out. Considering that a symmetrical sampled unipolar PWM produces a couple of twin pulses in each carrier period, the analysis framework is just half of carrier period and the calculation of the Fourier coefficients is carried out considering the pulse centered in $T_{\mathrm{PWM}}/2$ as a square waveform. Therefore, the fundamental frequency of the analyzed signal is $2f_{\mathrm{pwm}}$. Consequently, the overall ac multilevel output voltage produced every carrier period can be expressed as

$$v_0(t) = \sum_{i=1}^{N} \left(D_i V_i^{\mathrm{dc}} + \sum_{k=1}^{\infty} \frac{2V_i^{\mathrm{dc}}}{k\pi} \sin(k\pi D_i) \cos(k\omega t + k\varphi_i) \right) \tag{12}$$

where D_i is the ratio between the output voltage and the dc voltage of the ith converter.

The proposed technique consists in displacing, every PWM period, the carriers so that the fundamental harmonics ($2f_{\mathrm{pwm}}$) of the pulses of each H-bridge sum up to zero. Considering the case $N = 3$, the sum of the fundamental harmonics of the pulses produced by each bridge is null if the following condition is met:

$$\begin{cases} h_{11} + h_{12} \cos(\varphi_2) + h_{13} \cos(\varphi_3) = 0 \\ h_{12} \sin(\varphi_2) + h_{13} \sin(\varphi_3) = 0 \end{cases} \tag{13}$$

where

$$h_{ki} = \frac{2V_i^{\mathrm{dc}}}{k\pi} \sin(k\pi D_i) \tag{14}$$

are coefficients for H-bridge i and kth harmonic order, while $\varphi_2 = 2\theta_2$ and $\varphi_3 = 2\theta_3$ are, respectively, the displacement angles between the fundamental harmonics of the pulses of the second/third bridge and the fundamental harmonic of the pulses of the first bridge.

The solution to the equations in (13) is

$$\begin{aligned} \cos(\varphi_2) &= \frac{1}{2}\left(\frac{-h_{11}^2 - h_{12}^2 + h_{13}^2}{h_{11} h_{12}}\right) \\ \cos(\varphi_3) &= \frac{1}{2}\left(\frac{-h_{11}^2 + h_{12}^2 - h_{13}^2}{h_{11} h_{13}}\right). \end{aligned} \tag{15}$$

Valid solutions for the displacement angles φ_2 and φ_3 are obtained only if the following conditions are met:

$$\begin{aligned} |h_{11} - h_{12}| &\le h_{13} \le (h_{11} + h_{12}) \\ |h_{11} - h_{13}| &\le h_{12} \le (h_{11} + h_{13}). \end{aligned} \tag{16}$$

From (14) and (16) is evident that both the dc voltage values and the ratio D of each bridge deeply influence the validity region of this technique.

III. Comparison of the Technique Performances Under Different Unbalanced Conditions

Considering the case $N = 3$, the carrier phase shift angles θ_2 and θ_3 have been carried out for the techniques considered in the previous section under different unbalanced conditions. Such calculated values have been used to derive the theoretical harmonic spectra through the expressions presented in [1] for this multilevel converter in case of Techniques A and B. In fact, an exact analytical calculation of the harmonic components of a PWM waveform allows a precise determination of the harmonic characteristics and a more effective and rigorous comparison between PWM strategies. While, fast Fourier transform algorithm, although allowing expediency and reduced mathematical effort, produces results that could be affected by round-off or error due to its practical implementation. As regards Technique C, it calculates the value of the carrier phase shift angles θ_2 and θ_3 for every PWM period. Under unequal modulation indices conditions, the values θ_2 and θ_3 vary during a period of the modulating signal and hence a different theoretical harmonic spectrum can be achieved for each PWM period. For this reason, it is impossible to carry out a unique spectrum in this case, and hence, the harmonic performances of Technique C will be shown through experimental results.

A. Unequal DC Voltages and Equal Modulating Signals

To compare the performances of the three techniques under these unbalanced conditions, it has been considered

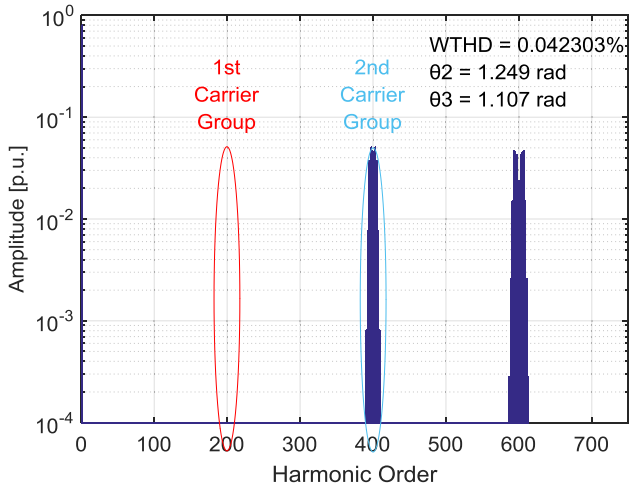

Fig. 3. Normalized theoretical harmonic spectra for all the three considered CPS-PWM techniques in case of unequal dc voltages and equal modulating signals.

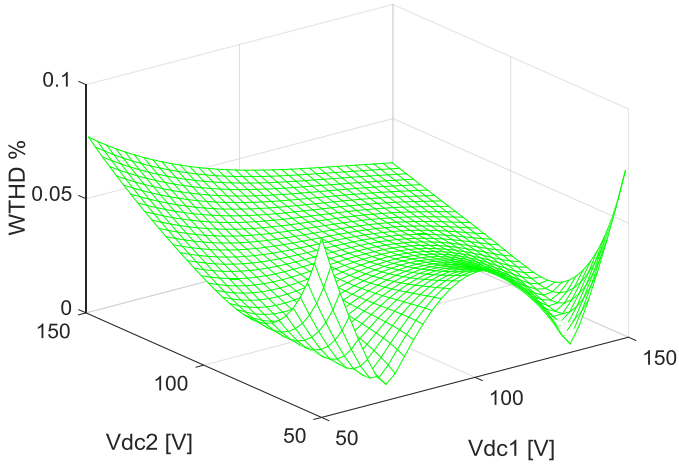

Fig. 4. WTHD trend as a function of V_1^{dc} and V_2^{dc} for $V_3^{\mathrm{dc}} =$ 100 V and M $=$ 0.8 for all the three considered CPS-PWM techniques.

$V_1^{\mathrm{dc}} = 100\,\mathrm{V}$, $V_2^{\mathrm{dc}} = 80\,\mathrm{V}$, $V_3^{\mathrm{dc}} = 60\,\mathrm{V}$, $f_{\mathrm{o}} = 50\,\mathrm{Hz}$, $f_c =$ 5000 Hz, and M $=$ 0.8.

Under these conditions, the three techniques are equivalent and hence produce the same harmonic spectrum shown in Fig. 3, although Technique A should still be preferred because of its lower computational burden. The mathematical demonstration of such an equivalence is included in the Appendix. From Fig. 3, it is possible to notice that the first carrier group is completely canceled out, although the second carrier group has not disappeared as it would happen in case of equal dc voltages with the conventional CPS-PWM. Fig. 4 shows the WTHD trend as a function of V_1^{dc} and V_2^{dc} for all the three considered CPS-PWM techniques. In particular is evident that its value increases as the degree of unbalance among the dc voltages of the three H-bridges increases.

B. Equal DC Voltages and Unequal Modulating Signals

To compare the performances of the three techniques under these unbalanced conditions it has been considered $V^{\mathrm{dc}} =$ 100 V, $f_{\mathrm{o}} = 50\,\mathrm{Hz}$, $f_c = 5000\,\mathrm{Hz}$, $M_1 = 0.5$, $M_2 = 0.7$, $\mathrm{M}_3 = 0.9$. In this case, the three techniques are not equivalent, and hence, different values of the carrier shifting angles are carried out.

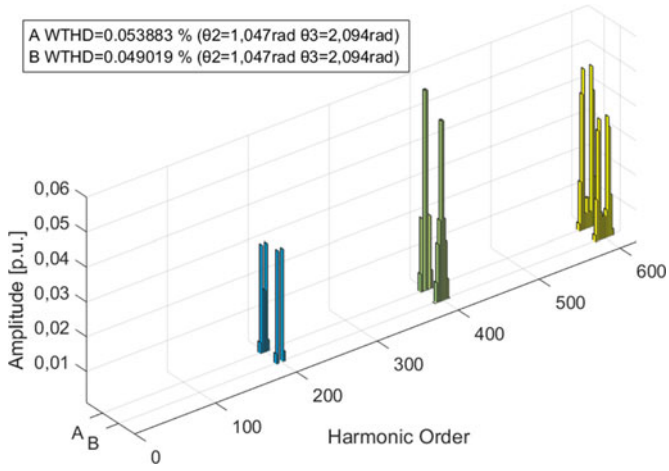

Fig. 5. Normalized theoretical harmonic spectra for Techniques A and B in case of equal dc voltages and unequal modulating signals.

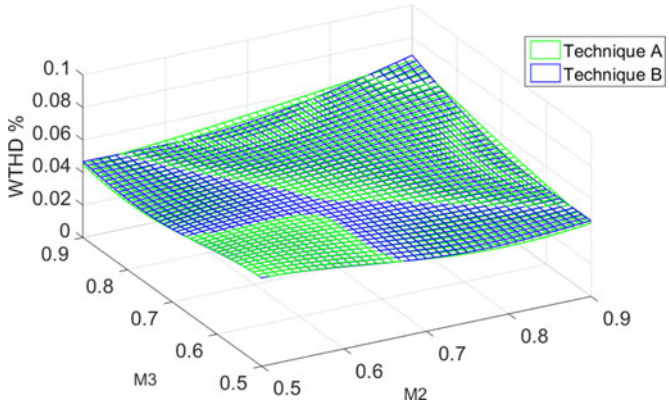

Fig. 6. WTHD trend as a function of M_2 and M_3 for $V^{\mathrm{dc}} =$ 100 V and $\mathrm{M}_1 = 0.5$ for Techniques A and B.

Fig. 5 shows that Technique A does not succeed in canceling the first carrier group anymore under these unbalanced conditions. Consequently, the WTHD value increases.

Technique B can cancel out the "main harmonics" in the first carrier group under these unbalanced conditions and, therefore, it can reduce the WTHD value.

Fig. 6 shows the WTHD trend as a function of M_2 and M_3 for Techniques A and B. It is possible to notice that the WTHD values almost the same.

C. Unequal DC Voltages and Unequal Modulating Signals

To compare the performances of the three techniques under these unbalanced conditions, it has been considered $V_1^{\mathrm{dc}} =$ 70 V, $V_2^{\mathrm{dc}} = 50\,\mathrm{V}$, $V_3^{\mathrm{dc}} = 40\,\mathrm{V}$, $f_{\mathrm{o}} = 50\,\mathrm{Hz}$, $f_c = 5000\,\mathrm{Hz}$, $M_1 = 0.95$, $M_2 = 0.9$, and $M_3 = 0.85$. Also in this case, the three techniques are not equivalent and hence different values of the carrier shifting angles are carried out. Fig. 7 shows that Technique A again does not succeed in canceling the first carrier group anymore under these unbalanced conditions. Moreover, it

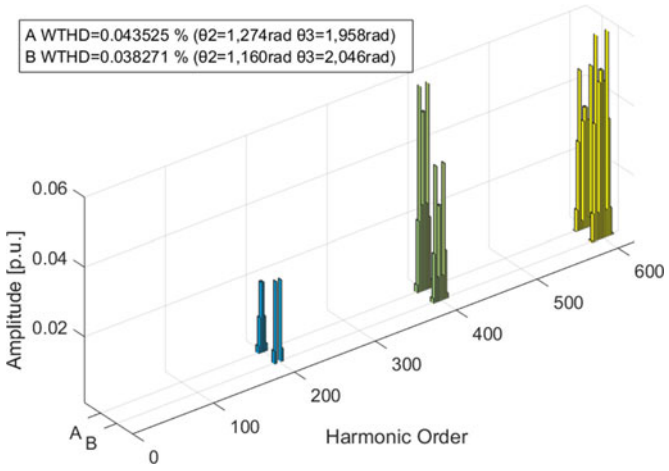

Fig. 7. Normalized theoretical harmonic spectra for Techniques A and B in case of unequal dc voltages and unequal modulating signals.

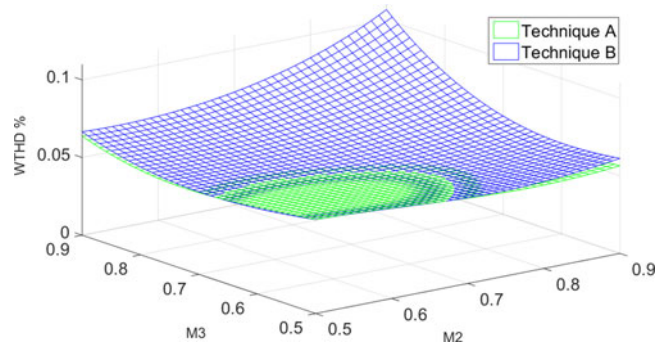

Fig. 8. WTHD trend as a function of M_2 and M_3 for $V_1^{\mathrm{dc}} = 100\,\mathrm{V}$, $V_2^{\mathrm{dc}} = 80\,\mathrm{V}$, $V_3^{\mathrm{dc}} = 60\,\mathrm{V}$ and $M_1 = 0.5$ for Techniques A and B.

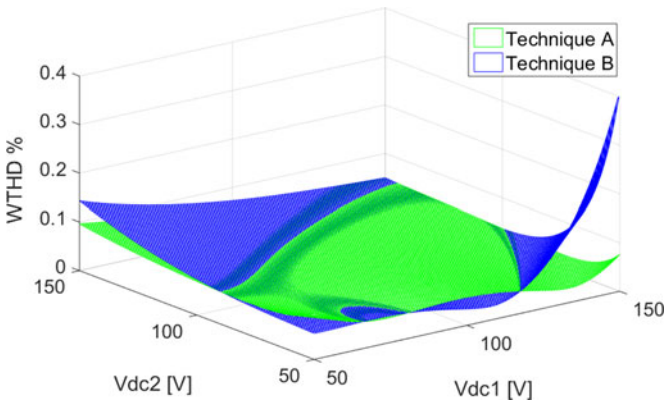

Fig. 9. WTHD trend as a function of V_1^{dc} and V_2^{dc} for $V_3^{\mathrm{dc}} = 100\,\mathrm{V}$, $M_1 = 0.5$, $M_2 = 0.7$, and $M_3 = 0.9$ for Techniques A and B.

can be noticed that Technique B again can cancel out the "main harmonics" in the first carrier group under these unbalanced conditions and, therefore, it performs a better WTHD value than Technique A. Fig. 8 shows the WTHD trend as a function of M_2 and M_3 for Techniques A and B. It is possible to notice that the WTHD values are almost the same. Fig. 9 shows the WTHD trend as a function of V_1^{dc} and V_2^{dc} for Techniques A and B. The two techniques perform almost equivalently unless when V_1^{dc} is much higher than V_2^{dc}. In this case, Technique A performs better.

D. Effects of the DC Voltage Second Harmonic Under Unbalanced Conditions.

The influence on the three considered techniques of a second harmonic (i.e., 100 Hz) in the dc voltage has been investigated by simulations in case of unequal dc voltages and equal modulating signals (case 1), in case of equal dc voltages and unequal modulating signals (case 2) and in case of unequal dc voltages and unequal modulating signals (case 3).

A ripple component of $5 * \sin(2 * \mathrm{pi} * 100 * t)$ [V] has been considered. As it can be seen in the frequency spectra (see Figs. 10–12) in case a second harmonic is present in the dc link, the output voltage has a third harmonic (i.e., 150 Hz). For case 1 (see Fig. 10), all techniques still manage to compensate the first harmonic group in case of a 100-Hz ripple in the dc voltage but their performance is diminished and the first group still appears.

For case 2 (see Fig. 11), Technique A already loses the ability with the pure dc voltage. The main effect of Technique B is to cancel out the harmonics $2m_f \pm 1$ (the components indicated with arrow). However, the components are not completely eliminated when a second harmonic is present in the dc voltage. On the other hand, Technique C shows a similar performance also in presence of a second harmonic.

For case 3 (see Fig. 12), the Techniques A and B show a behavior similar to the previous case 2. The performance of Technique C decreases due to the second harmonics in the dc voltage, showing harmonics belonging to the first group.

IV. Experimental Results

In the following, the three considered PSC-PWM techniques are tested on a developed prototype shown in Fig. 13, considering unbalanced operating conditions. The developed prototype is composed of the seven-level CHB converter with discrete IGBTs (IXYB82N120C3H1), a microprocessor (MPC5643L) to implement the techniques and to generate the gating signals, and three isolated dc sources to emulate the unequal dc voltage cases considered in the analysis section. The experimental test conditions are identical to those considered for simulations.

A. Unequal DC Voltages and Equal Modulating Signals

Under these operating conditions, the symmetrical PSC-PWM presents an increased WTHD value of 0.0569%. On the other hand, by means of all three PSC-PWM techniques (see Fig. 14), the first carrier group is canceled out while the second carrier group is increasing. Hence, these techniques achieve the reduced WTHD of 0.0447%. All the three techniques allow a WTHD improvement of 21.44% compared to the symmetrical PSC-PWM technique. It should be noted that the carrier shifting angles calculated by each technique are same as $\theta_2 = 1.249$ rad and $\theta_3 = 1.107$ rad since three techniques are equivalent under the unequal dc voltages and equal modulating signals as mentioned in Section III-A.

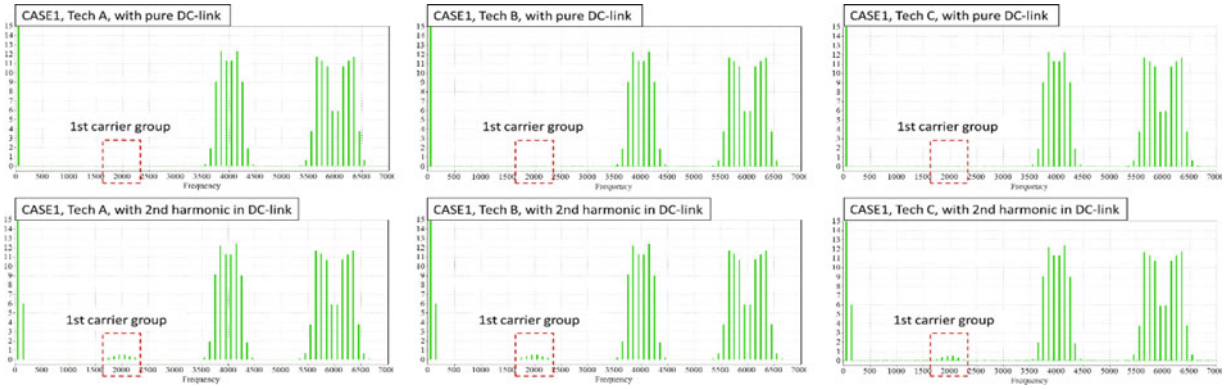

Fig. 10. Frequency spectra of inverter output voltage produced by the three considered techniques in case of unequal dc voltages and equal modulating signals (case 1) without second harmonic in the dc link (up) and with second harmonic in the dc link (down).

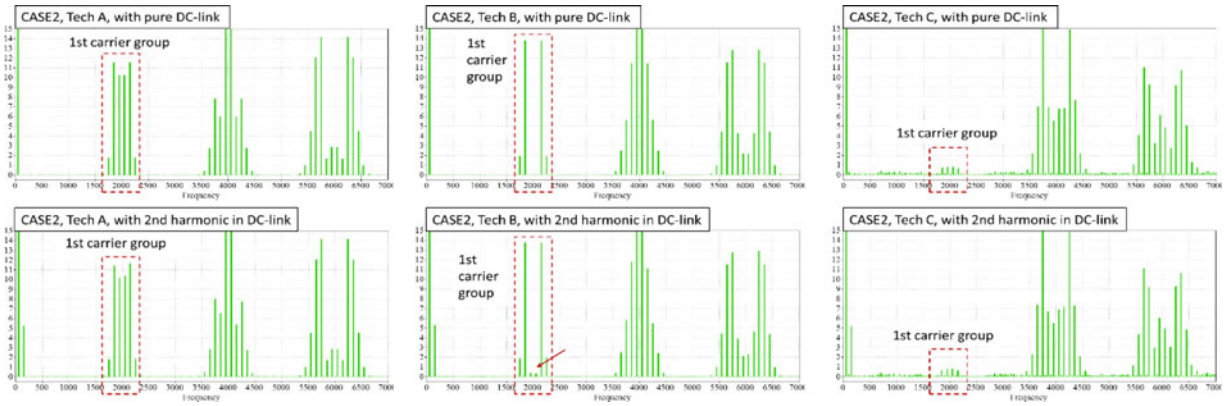

Fig. 11. Frequency spectra of inverter output voltage produced by the three considered techniques in case of equal dc voltages and unequal modulating signals (case 2) without second harmonic in the dc link (up) and with second harmonic in the dc link (down).

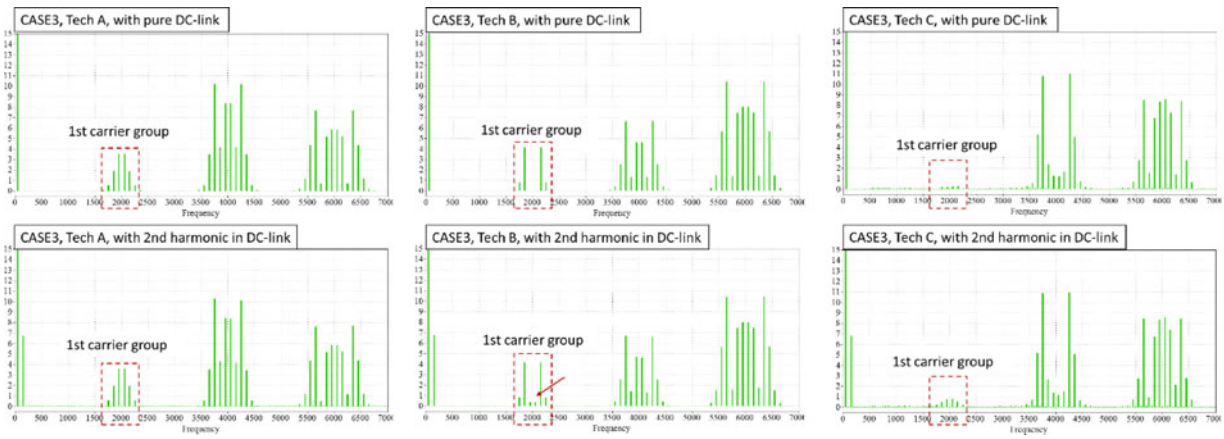

Fig. 12. Frequency spectra of inverter output voltage produced by the three considered techniques in case of unequal dc voltages and unequal modulating signals (case 3) without second harmonic in the dc link (up) and with second harmonic in the dc link (down).

B. Equal DC Voltages and Unequal Modulating Signals

Under these operating conditions, the symmetrical PSC-PWM presents an increased WTHD value of 0.0668%. The effect of each technique is identified and these are shown in Figs. 15–17, respectively.

Technique A does not influence on the carrier angle and the WTHD at all under this condition as shown in Fig. 15. In fact, its WTHD value is identical with that of the symmetrical PSC-PWM.

Technique B makes the main harmonics in the first carrier group to diminish in part. The decreased main harmonics

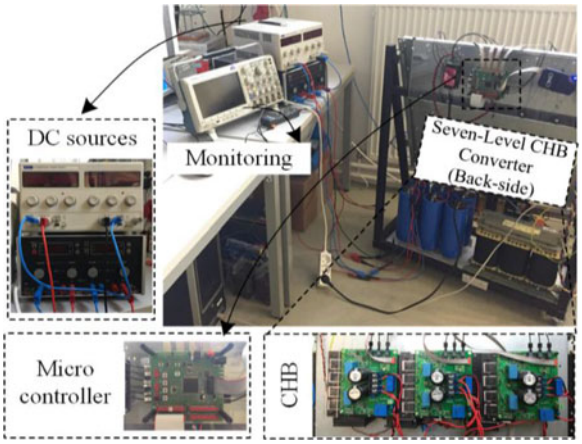

Fig. 13. Experimental setup.

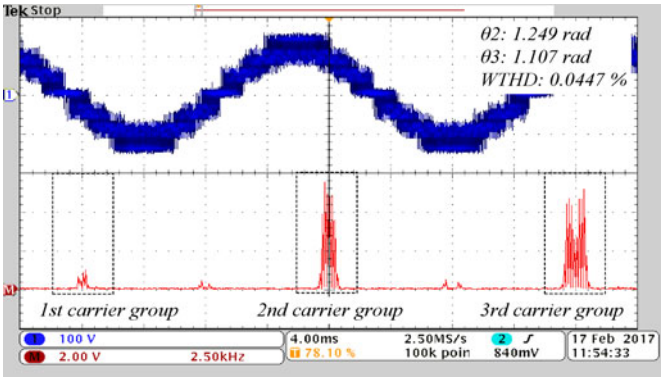

Fig. 14. Experimental converter voltage and its harmonic spectrum with PSC-PWM Techniques A, B, and C in case of unequal dc voltages and equal modulating signals.

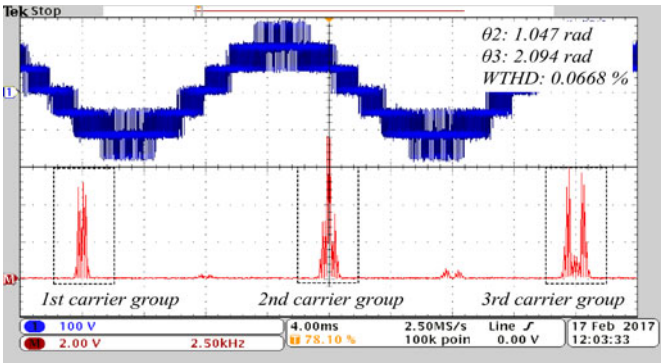

Fig. 15. Experimental converter voltage and its harmonic spectrum with PSC-PWM Technique A in case of equal dc voltages and unequal modulating signals.

are $2m_f \pm 1$, where m_f is the frequency modulation index (5 kHz/50 Hz $=$ 100). Hence, the WTHD decreases to 0.0613% and it is 8.23% lower than that of symmetrical PSC-PWM.

However, the WTHD of Technique C is the best one since the harmonics of $2m_f \pm 1$ are remarkably decreasing. Therefore, considering the equal dc voltages and the unequal modulating signals conditions, Technique C achieves the best performance since its WTHD is 43.41% lower than that of symmetrical PSC-PWM.

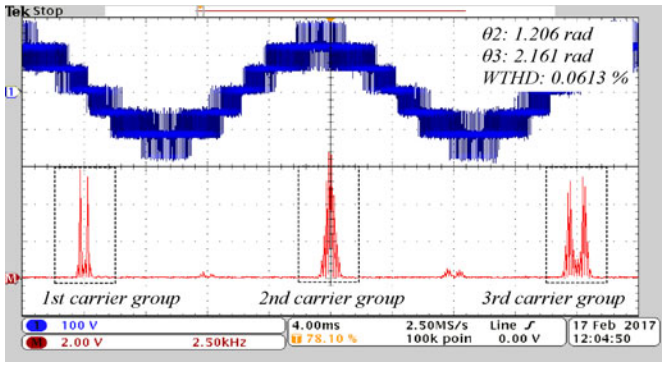

Fig. 16. Experimental converter voltage and its harmonic spectrum with PSC-PWM Technique B in case of equal dc voltages and unequal modulating signals.

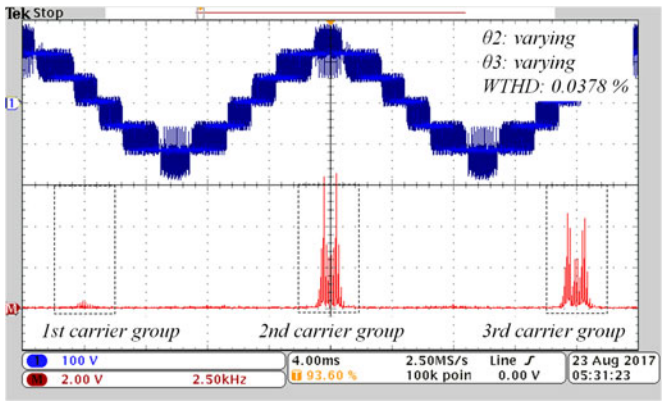

Fig. 17. Experimental converter voltage and its harmonic spectrum with PSC-PWM Technique C in case of equal dc voltages and unequal modulating signals.

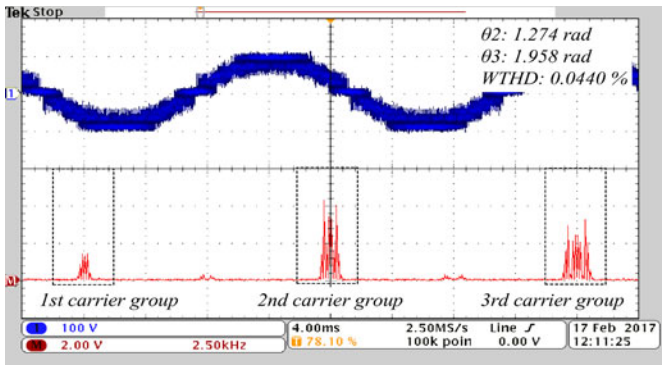

Fig. 18. Experimental converter voltage and its harmonic spectrum with PSC-PWM Technique A in case of unequal dc voltages and unequal modulating signals.

C. Unequal DC Voltages and Unequal Modulating Signals

Under these operating conditions, the WTHD is 0.0479% with the symmetrical PSC-PWM. Technique A improves the WTHD value to 0.044% since harmonics of the first carrier group are attenuated (see Fig. 18). Fig. 19 shows the waveforms with Technique B that reduces effectively the harmonics of $2m_f \pm 1$, resulting in the improved performance of 0.0406%. Technique C allows the harmonics of $2m_f \pm 1$ to diminish

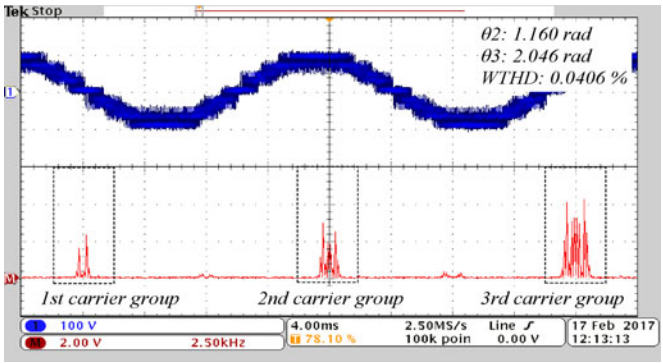

Fig. 19. Experimental converter voltage and its harmonic spectrum with PSC-PWM Technique B in case of unequal dc voltages and unequal modulating signals.

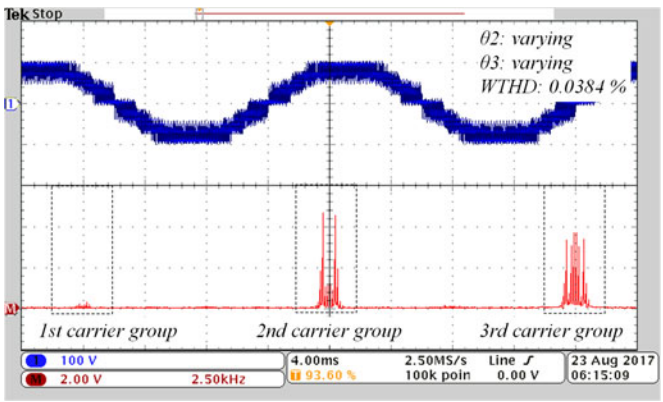

Fig. 20. Experimental converter voltage and its harmonic spectrum with PSC-PWM Technique C in case of unequal dc voltages and unequal modulating signals.

without increasing the $2m_f \pm 3$, such as the previous case and the WTHD is 0.0384% (see Fig. 20). All techniques can improve the WTHD performance compared to the symmetrical PSC-PWM technique. For Technique A, the WTHD is improved by 8.14%, whereas for Techniques B and C, it is improved by 15.24% and 19.83%, respectively.

V. Conclusion

In this paper, three different variations to the conventional symmetrical CPS-PWM technique, to be used in case of unbalanced operational conditions, were compared and their performances were analyzed. To uniquely assess their performances, the techniques were tested in the same unbalanced conditions and their spectra as well as the WTHD were evaluated. Moreover, experimental tests were carried out on a seven-level CHB converter and the three techniques were verified in terms of the WTHD for the different unbalanced conditions. Experimental results showed a good agreement with the outcomes of the theoretical analysis. In particular, the effect of all the techniques was equal in case of unequal dc voltages and equal modulating signals, whereas the minimum WTHD was achieved by Technique C under equal/unequal dc voltages and unequal modulating signals. In conclusion, this paper provided an effective mean to select the most suitable carrier phase-shifting PWM technique to be profitably used under different unbalanced conditions.

Appendix

Considering unequal dc voltages and equal modulating signals (i.e., $M_1 = M_2 = M_3 = M$), Technique B is equivalent to Technique A since

$$\cos\varphi_2 = \frac{V_3^2 - V_1^2 - V_2^2}{2V_1V_2}$$

$$= \frac{\left(-\frac{2V_{\mathrm{dc},3}}{\pi}J_1(\pi M_3)\right)^2 - \left(-\frac{2V_{\mathrm{dc},1}}{\pi}J_1(\pi M_1)\right)^2 - \left(-\frac{2V_{\mathrm{dc},2}}{\pi}J_1(\pi M_2)\right)^2}{2\left(-\frac{2V_{dc,1}}{\pi}J_1(\pi M_1)\right)\left(-\frac{2V_{dc,2}}{\pi}J_1(\pi M_2)\right)}$$

$$= \frac{\frac{4}{\pi^2}J_1^2(\pi M)\left(V^2{}_{\mathrm{dc},3} - V^2{}_{\mathrm{dc},1} - V^2{}_{\mathrm{dc},2}\right)}{2\frac{4}{\pi^2}J_1^2(\pi M)V_{\mathrm{dc},1}V_{\mathrm{dc},2}}$$

$$= \frac{V^2{}_{\mathrm{dc},3} - V^2{}_{\mathrm{dc},1} - V^2{}_{\mathrm{dc},2}}{2V_{\mathrm{dc},1}V_{\mathrm{dc},2}}.$$

Similarly

$$\cos\varphi_3 = \frac{V_2^2 - V_1^2 - V_3^2}{2V_1V_3} = \frac{{V_{\mathrm{dc},2}}^2 - {V_{\mathrm{dc},1}}^2 - {V_{dc,3}}^2}{2V_{\mathrm{dc},1}V_{\mathrm{dc},3}}.$$

Considering unequal dc voltages and equal modulating signals (i.e., $M_1 = M_2 = M_3 = M$ and hence $D_1 = D_2 = D_3 = D$), Technique C is equivalent to Technique A since

$$\cos\varphi_2 = \frac{h_{13}^2 - h_{11}^2 - h_{12}^2}{2h_{11}h_{12}}$$

$$= \frac{\left(\frac{2V_{\mathrm{dc},3}}{\pi}\sin(\pi D_3)\right)^2 - \left(\frac{2V_{\mathrm{dc},1}}{\pi}\sin(\pi D_1)\right)^2 - \left(\frac{2V_{\mathrm{dc},2}}{\pi}\sin(\pi D_2)\right)^2}{2\left(\frac{2V_{\mathrm{dc},1}}{\pi}\sin(\pi D_1)\right)\left(\frac{2V_{\mathrm{dc},2}}{\pi}\sin(\pi D_2)\right)}$$

$$= \frac{\frac{4}{\pi^2}\sin^2(\pi D)\left(V^2{}_{\mathrm{dc},3} - V^2{}_{\mathrm{dc},1} - V^2{}_{\mathrm{dc},2}\right)}{2\frac{4}{\pi^2}\sin^2(\pi D)V_{\mathrm{dc},1}V_{\mathrm{dc},2}}$$

$$= \frac{V^2{}_{\mathrm{dc},3} - V^2{}_{\mathrm{dc},1} - V^2{}_{\mathrm{dc},2}}{2V_{\mathrm{dc},1}V_{\mathrm{dc},2}}.$$

Similarly

$$\cos\varphi_3 = \frac{h_{12}^2 - h_{11}^2 - h_{13}^2}{2h_{11}h_{13}} = \frac{{V_{\mathrm{dc2}}}^2 - {V_{\mathrm{dc1}}}^2 - {V_{\mathrm{dc3}}}^2}{2V_{\mathrm{dc1}}V_{\mathrm{dc3}}}.$$

References

[1] L. M. Tolbert, J. N. Chiasson, Z. Du, and K. J. McKenzie, "Elimination of harmonics in a multilevel converter with non equal DC sources," *IEEE Trans. Ind. Appl.*, vol. 41, no. 1, pp. 75–82, Jan./Feb. 2005.

[2] F. Filho, H. Z. Maia, T. H. A. Mateus, L. M. Tolbert, B. Ozpineci, and J. O. P. Pinto, "Adaptive selective harmonic minimization based on ANNs for cascade multilevel inverters with varying DC sources," *IEEE Trans. Ind. Electron.*, vol. 60, no. 5, pp. 1955–1962, May 2013.

[3] D. Holmes and T. Lipo, *Pulse Width Modulation for Power Converters: Principles and Practice*. Hoboken, NJ, USA: Wiley, 2003.

[4] A. Dell'Aquila, M. Liserre, V. G. Monopoli, and P. Rrotondo, "Overview of PI-based solutions for the control of DC buses of a single-phase H-bridge multilevel active rectifier," *IEEE Trans. Ind. Appl.*, vol. 44, no. 3, pp. 857–866, May 2008.

[5] Y. Sun, J. Zhao, and Z. Ji, "An improved CPS-PWM method for cascaded multilevel STATCOM under unequal losses," in *Proc. 39th Annu. Conf. IEEE Ind. Electron. Soc.*, Vienna, Austria, Nov. 10–13, 2013, pp. 418–423.

[6] J. A. Barrena, L. Marroyo, M. A. R. Vidal, and J. R. T Apraiz, "Individual voltage balancing strategy for PWM cascaded H-bridge converter based STATCOM," *IEEE Trans. Ind. Electron.*, vol. 55, no. 1, pp. 21–29, Jan. 2008.

[7] D. Soto, R. Pena, and P. Wheeler, "Decoupled control of capacitor voltages in a PWM cascade StatCom," in *Proc. 39th Annu. Conf. IEEE Power Electron. Spec. Conf.*, Jun. 15–19, 2008, pp. 1384–1389.

[8] S. Kouro *et al.*, "Recent advances and industrial applications of multilevel converters," *IEEE Trans. Ind. Electron.*, vol. 57, no. 8, pp. 2553–2580, Aug. 2010.
[9] X. M. Zha, L. Xiong, J. W. Gong, and F. Liu, "Cascaded multilevel converter for medium-voltage motor drive capable of regenerating with part of cells," *IET Power Electron.*, vol. 7, no. 5, pp. 1313–1320, 2014.
[10] B. Xiao, L. Hang, J. Mei, C. Riley, L. M. Tolbert, and B. Ozpineci, "Modular cascaded H-bridge multilevel PV inverter with distributed MPPT for grid-connected applications," *IEEE Trans. Ind. Appl.*, vol. 51, no. 2, pp. 1722–1731, Mar. 2015. doi: 10.1109/TIA.2014.2354396.
[11] E. Villanueva, P. Correa, J. Rodriguez, and M. Pacas, "Control of a single-phase cascaded H-bridge multilevel inverter for grid-connected photovoltaic systems," *IEEE Trans. Ind. Electron.*, vol. 56, no. 11, pp. 4399–4406, Nov. 2009. doi: 10.1109/TIE.2009.2029579.
[12] L. Liu, H. Li, Z. Wu, and Y. Zhou, "A cascaded photovoltaic system integrating segmented energy storages with self-regulating power allocation control and wide range reactive power compensation," *IEEE Trans. Power Electron.*, vol. 26, no. 12, pp. 3545–3559, Dec. 2011. doi: 10.1109/TPEL.2011.2168544.
[13] M. Liserre, V. G. Monopoli, A. Dell'Aquila, A. Pigazo, and V. Moreno, "Multilevel phase-shifting carrier PWM technique in case of non-equal dc-link voltages," in *Proc. 32nd Annu. Conf. IEEE Ind. Electron.*, Nov. 2006, pp. 1639–1642. doi: 10.1109/IECON.2006.347669.
[14] S. Li, Z. Yang, Q. Li, J. Gong, J. Sun, and X. Zha, "Asymmetrical phase-shifting carrier pulse-width modulation for harmonics suppression in cascaded multilevel converter under unbalanced DC-link voltages," in *Proc. 2015 IEEE Energy Convers. Congr. Expo.*, Montreal, Canada, Sep. 20–24, 2015, pp. 6804–6810.
[15] Y. Sun, J. Zhao, and Z. Ji, "An improved CPS-PWM method for cascaded multilevel STATCOM under unequal losses," in *Proc. IECON 39th Annu. Conf. IEEE Ind. Electron. Soc.*, Vienna, Austria, Nov. 10–13, 2013, pp. 418–423.
[16] A. Marquez *et al.*, "Variable-angle phase-shifted PWM for multilevel three-cell cascaded H-bridge converters," *IEEE Trans. Ind. Electron.*, vol. 64, no. 5, pp. 3619–3628, May 2017. doi: 10.1109/TIE.2017.2652406.

Vito Giuseppe Monopoli (S'98–M'05) received the M.Sc. and Ph.D. degrees in electrical engineering from the Bari Polytechnic, Bari, Italy, in 2000 and 2004, respectively.

He is currently an Assistant Professor with Bari Polytechnic. His research interests include multilevel converters and the analysis of harmonic distortion produced by power converters and electrical drives. He is particularly interested in innovative control techniques for power converters.

Dr. Monopoli is a member of the IEEE Industry Applications Society, the IEEE Industrial Electronics Society, and the IEEE Power Electronics Society.

Youngjong Ko (S'16) received the B.Sc. and M.Sc. degrees in electronic engineering from the Ajou University, Suwon, South Korea, in 2009 and 2012, respectively. He is currently working toward the Ph.D. degree in reliability in power electronics at the Chair of Power Electronics, University of Kiel, Kiel, Germany.

His research interests include grid-connected power converter and reliability in power electronics.

Giampaolo Buticchi (S'10–M'13–SM'17) received the master's degree in electronic engineering and Ph.D degree in information technologies from the University of Parma, Parma, Italy, in 2009 and 2013, respectively.

In 2012, he was a Visiting Researcher with The University of Nottingham, Nottingham, U.K. Between 2014 and 2017, he was a Postdoctoral Researcher with the University of Kiel, Germany. He is currently an Associate Professor with the Department of Electrical Engineering, The University of Nottingham Ningbo China, Ningbo, China. He is the author/coauthor of more than 120 scientific papers. His research interests include power electronics for renewable energy systems, smart transformer fed microgrids, and dc grids for the more electric aircraft.

Marco Liserre (S'00–M'02–SM'07–F'13) received the M.Sc. and Ph.D. degrees in electrical engineering from the Bari Polytechnic, Bari, Italy, in 1998 and 2002, respectively.

He is currently a Full Professor and the Head of the Chair of Power Electronics, University of Kiel, Kiel, Germany. He is the author of more than 300 technical papers, which received more than 20 000 citations. He has authored or coauthored more than 200 technical papers (one third in international peer-reviewed journals) and a book in its second reprint and also translated in Chinese. These works have received more than 15 000 citations, for this reason, he is listed in ISI Thomson report "The world's most influential scientific minds" from 2014.

Prof. Liserre was the recipient of the European ERC Consolidator Grant, one of the most prestigious in Europe, and several IEEE Awards. He is a member of the IEEE Industrial Applications Society, the IEEE Power Electronics Society, the IEEE Power and Energy Society, and the IEEE Industrial Electronics Society. He did serve all these societies in various capacities, such as a Reviewer, an Associate Editor, an Editor, a Conference Chairman, or a Track Chairman. He has been a Founding Editor-in-Chief for the IEEE INDUSTRIAL ELECTRONICS MAGAZINE, a Founding Chairman of the Technical Committee on Renewable Energy Systems, and the IES Vice-President responsible for the publications.